Thermodynamic and Density Functional Theory Investigation of Sulphathiazole as Green Corrosion Inhibitor at Mild Steel/Hydrochloric Acid Interface

I.B. Obot[1,], E.E. Ebenso[2], I. A. Akpan[1], Z. M. Gasem[3], Ayo S. Afolabi[4]*

[1] Department of Chemistry, Faculty of Science, University of Uyo, P.M.B 1017, Uyo, Akwa Ibom State, Nigeria.
[2] Department of Chemistry, School of Mathematical and Physical Sciences, North-West University (Mafikeng Campus), Private Bag X2046, Mmabatho 2735, South Africa
[3] Department of Mechanical Engineering, King Fahd University of Petroleum and Minerals, Dhahran, Saudi Arabia.
[4] Department of Civil and Chemical Engineering, University of South Africa, Florida Campus, Johannesburg, South Africa
[*]E-mail: proffoime@yahoo.com

The corrosion inhibition efficiency of sulphathiazole (STZ) on mild steel in 0.5 M HCl at 303-333 K was studied using gravimetric and quantum chemical methods. Results show that STZ acts as inhibitor for steel corrosion even at very low concentration. The adsorption of STZ on steel surface obeyed the Temkin adsorption isotherm. The kinetic and thermodynamic parameters for mild steel corrosion and inhibition adsorption, respectively, were determined and discussed. The calculated activation and Gibbs free energy values confirm the chemical nature of the adsorption process. It is most probable that the inhibition property of STZ was due to charge sharing between the inhibitor molecules and the metal surface. Attempt were made to correlate the structural and electronic properties such as E_{HOMO}, E_{LUMO}, Energy gap, Mulliken charges, HOMO and LUMO orbitals using density functional theory (DFT) at the BLYP/6-31G(d) basis set with the inhibitive action of STZ.

1. INTRODUCTION

The use of inhibitor is one of the best known methods of corrosion protection of steel. The efficiency of inhibitor depends on the nature of environment, nature of metal surface, electrochemical potential at the interface, and the structural feature of inhibitor, which includes number of adsorption

centers in the molecule, their charge density, the molecular size, and mode of adsorption, formation of metallic complexes and the projected area of inhibitor on the metal surface [1]. Organic compounds containing hetero-atoms such as N, O, and S have been reported as efficient inhibitors for metals and alloys [2-4]. Among various heterocyclic compounds, molecules containing both N and S provide excellent inhibition activity compared to those containing only N or S [5-7]. In spite of the presence of all these favouring factors, inhibition efficiency of many organic inhibitors generally decreases with an increase in temperature. But, usually acid pickling is carried out at higher temperature [8]. Hence it is important to find inhibitor which has fair inhibition efficiency at elevated temperature. It has been reported that chemisorption is responsible for retaining the inhibition efficiency at elavated temperature. [9, 10]. Other researchers showed that the planarity of the molecule besides other factors plays an important role in retaining efficiency at high temperature [11, 12].

In the past two decade, the research in the field of ''green'' corrosion inhibitors has been directed towards the goal of using cheap, effective molecules of low or ''zero'' negative environmental impact. Therefore, the use of non-toxic inhibitors has also become one of the major selection requirements [13-15]. Unfortunately, many common corrosion inhibitors that are still in use today are harzardous to health [16]. Therefore, there is still an increased attention directed towards the development of environmentally compatible, nonpolluting corrosion inhibitors. Thus, in recent years, alternative eco-friendly corrosion inhibitors have been developed. They range from rare earth elements [17], to organic compounds such as amino acids [18-20], and drugs [21-23]. The review including extensive listing of various classes of drugs as corrosion inhibitors has recently been published [24]. The focus of a part of our research is to study the feasibility of application of non-toxic organic compounds such as drugs as good inhibitors in various corrosive solutions. The interesting results obtained recently in our laboratories for drugs such as fluconazole [25], ketoconazole [26] and clotrimazole [27] as inhibitors for metal corrosion in acid solutions have incited us to use another drug (sulphathiazole) as steel corrosion inhibitor in HCl solution.

Sulphathiazole which belongs to a class of drugs known as sulphonamides are extensively used for the treatment of infections caused by gram-positive microorganisms, some fungi, and certain protozoa. Although the advent of antibiotics has diminished the usefulness of sulfonamides, they still occupy a relatively small, but important place in the therapeutic resources for physicians. Other therapeutic uses of sulfonamides are as diuretic and hypoglycemic agents. These compounds have a large number of functional adsorption centers (e.g. $-NH_2$ group, $-SO_2-NH-$ group, O and/or N heteroatoms and aromatic rings). They are strongly basic hence they can be readily soluble in the acid medium which is an important requirement for a good corrosion inhibitor [28]. In continuation of our program for the development of corrosion inhibitors with high effectiveness and efficiency, the present paper explore the use of sulphathiazole as safe corrosion inhibitor for steel corrosion in HCl solutions using gravimetric technique. The effect of temperature (303-333 K) on corrosion and inhibition processes are thoroughly assessed and discussed. Thermodynamic parameters governing the adsorption process were also calculated and discussed. Quantum chemical study using density functional theory (DFT) at the BLYP/6-31G(d) method was further employed in an attempt to correlate the inhibitive effect with the molecular/electronic properties of sulphathiazole.

2. EXPERIMENTAL DETAILS

Tests were performed on a freshly prepared sheet of mild steel of the following composition (wt. %): 0.13% C, 0.18% Si, 0.39% Mn, 0.40% P, 0.04% S, 0.025% Cu, and bal. Fe. Specimens used in the weight loss experiment were mechanically cut into 5.0 cm x 4.0 cm x 0.8 cm dimensions, then abraded with SiC abrasive papers 320, 400 and 600 grit respectively, washed in absolute ethanol and acetone, dried in room temperature and stored in a moisture free dessicator before their use in corrosion studies [29]. The aggressive solutions, 0.5 M HCl were prepared by dilution of analytical grade HCl with distilled water. Sulphathiazole was obtained commercially from Amela Pharmaceutical Company in Nigeria. Stock solution of STZ was made in 10:1 water: methanol mixture to ensure solubility [30]. This stock solution was used for all experimental purposes. The concentration range of STZ prepared and used in this study was 0.4 µM − 1.0 µM. Fig. 1 depicts the name and molecular structure of STZ.
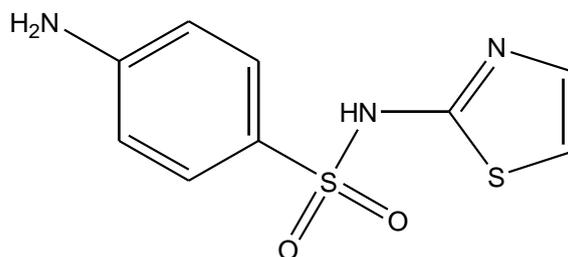

Figure 1. IUPAC name and molecular structure of Sulphathiazole.

Weight loss measurements were conducted under total immersion using 250 mL capacity beakers containing 200 mL test solution at 303-333 K maintained in a thermostated water bath. The mild steel coupons were weighed and suspended in the beaker with the help of rod and hook. The coupons were retrieved at 2 h interval progressively for 10 h at 303 K and 2 h at 313-333 K, washed thoroughly in 20% NaOH solution containing 200 g/l of zinc dust [31] with bristle brush, rinsed severally in deionized water, cleaned, dried in acetone, and re-weighed. The weight loss, in grammes, was taken as the difference in the weight of the mild steel coupons before and after immersion in different test solutions determined using LP 120 digital balance with sensitivity of ± 0.1 mg. Then the tests were repeated at different temperatures. In order to get good reproducibility, experiments were carried out in triplicate. In this present study, the standard deviation values among parallel triplicate experiments were found to be smaller than ± 2 %, indicating good reproducibility.

The corrosion rate (ρ) in g cm^{-2} h^{-1} was calculated from the following equation [29]:

$$\rho = \frac{\Delta W}{At} \tag{1}$$

where W is the average weight loss of three mild steel sheets, *A* the total area of one mild steel specimen, and t is the immersion time . With the calculated corrosion rate, the inhibition efficiency *(%I)* was calculated as follows [31]:

$$\%I = \left(\frac{\rho_1 - \rho_2}{\rho_1} \right) x100 \tag{2}$$

Where ρ_1 and ρ_2 are the corrosion rates of the mild steel coupons in the absence and presence of inhibitor, respectively.

3. RESULTS AND DISCUSSION

3.1. Weight loss, corrosion rates and inhibition efficiency

The gravimetric method (weight loss) is probably the most widely used method of inhibition assessment [32]. The simplicity and reliability of the measurement offered by the weight loss method is such that the technique forms the baseline method of measurement in many corrosion monitoring programmes [33]. Several authors have reported on comparable agreement between weight loss technique and other well established techniques of corrosion monitoring such as polarization technique [34], electrochemical impedance spectroscopy [35], gasometric [36], thermometric [37] and atomic absorption spectroscopy [38]. Recently, weight loss method together with potentiodynamic polarization and electrochimical impedance spectroscopy were used to evaluate the corrosion inhibitive effect of cigarette butt on N80 steel at 90 ^{o}C in hydrochloric acid solution [39]. Results obtained for the three independent methods were in good agreement. The weight loss method in combination with quantum chemical studies has been found to be adequate in elucidating the mechanism of inhibition [26-31].

Weight loss of mild steel was determined at various time intervals in absence and presence of different concentrations of STZ at 303 – 333 K (Table 1).

Table 1. Calculated values of corrosion rate and inhibition efficiency for mild steel corrosion in 0.5 M HCl in the absence and presence of STZ at 303-333K

System/concentration	Corrosion rate (mg cm^{-2} h^{-1})				Inhibition efficiency (%I)			
	303K	313K	323K	333K	303K	313K	323K	333K
Blank	2.73	11.14	12.23	13.07	-	-	-	-
0.4 mM	1.42	5.30	5.65	5.83	47.9	52.4	53.8	55.4
0.6 mM	1.26	4.95	5.20	5.37	53.6	55.5	57.4	58.8
0.8 mM	1.15	4.42	4.57	4.83	57.5	60.3	62.6	63.3
1.0 mM	1.00	3.83	4.12	4.31	63.1	65.3	66.3	70.0

The obtained weight loss-time curves at 303 K for 2 – 10 h immersion time is presented in Fig. 2.
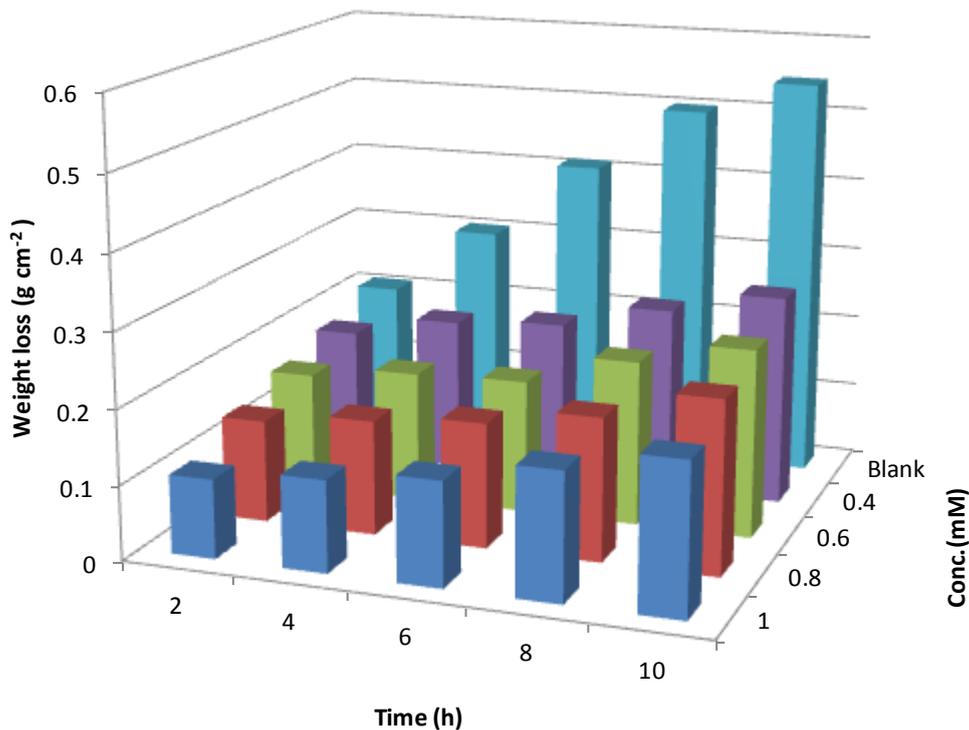

Figure 2. Variation of weight loss against time for mild steel corrosion in 0.5 M HCl in the   presence of different concentrations of STZ at 303 K.
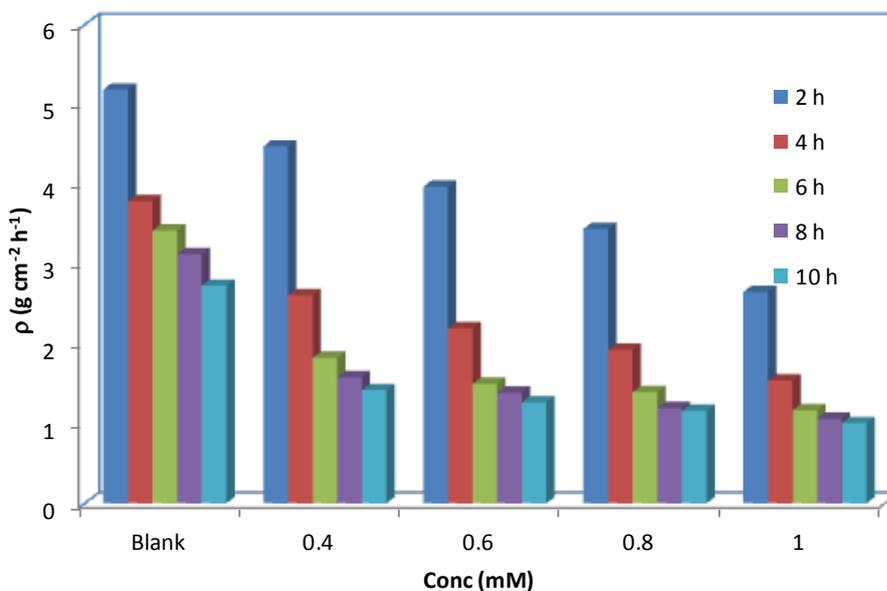

Figure 3. The relationship between corrosion rate and concentrations of STZ at different immersion time at 303 K.
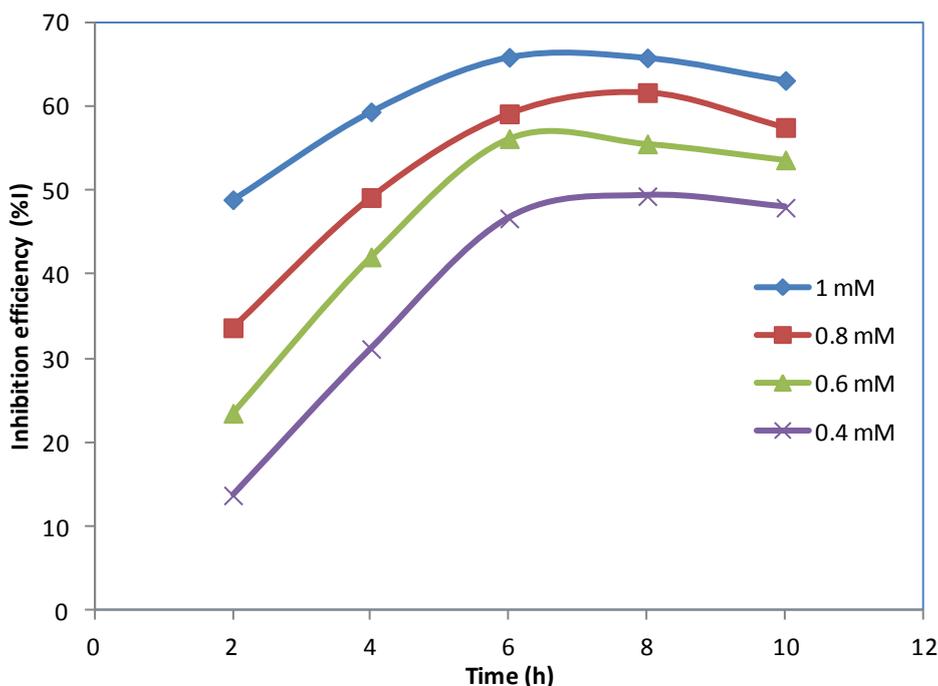
Figure 4. Variation of inhibition efficiency of STZ with time at 303 K.

It is clear from the figure that the weight loss obtained in the presence of the inhibitor is lower than that obtained in the free acid solution (blank). It is also clear that the increase in the inhibitor concentration was accompanied by a decrease in weight loss and an increase in the percentage inhibition efficiency.

In order to assess the stability of inhibitive behaviour of STZ on a time scale, corrosion rates and inhibition efficiencies were plotted against immersion time as presented in Figs. 3 and 4 respectively. Fig. 3 shows that corrosion rate decreased with increase in immersion time at all the concentration studied while Fig.4 shows that inhibition efficiency of STZ increased with time up to a maximum of 6 h and remains fairly constant till 10 h due to the strong adsorption of STZ on the mild steel surface. This resulted in a more protective layer formed at mild steel/hydrochloric acid solution interface. Thus, STZ effectively inhibits the mild steel corrosion in hydrochloric acid solution. These results lead to the conclusion that STZ is fairly efficient as inhibitor for mild steel dissolution in hydrochloric acid solution. Similar report has been documented previously [40].

3.2. Effect of temperature and activation energy

The effect of temperature on the inhibited acid-metal reaction is highly complex, because many changes occur on the metal surface such as rapid etching, desorption of the inhibitor, and the inhibitor may undergo decomposition and/or rearrangement. To evaluate the effect of temperature on the adsorption behaviour as well as the activation parameters of the corrosion processes of mild steel in 0.5 M HCl in the blank solution and solutions containing STZ, the weight loss measurements were carried out in the temperature range of 303 – 333 K. The influence of temperature on the inhibition efficiency

at different concentrations of STZ is illustrated in Table 1. It is evident from this table that inhibition efficiency increases with increasing temperature. This is due to decreased rate of dissolution process of mild steel and strong adsorption of the inhibitor onto the metal surface with temperature [41]. The relationship between the corrosion rate (ρ) of mild steel in acidic media and temperature (T) is often expressed by the Arrhenius equation [42]:

$$\log \rho = \log A - \frac{E_a}{2.303RT} \qquad (3)$$

where ρ is the corrosion rate E_a is the apparent activation energy, R is the molar gas constant (8.314 *J K^{-1} mol^{-1}*), T is the absolute temperature, and A is the frequency factor. The plot of *log ρ* against *1/T* for mild steel corrosion in 0.5 M HCl in the absence and presence of different concentrations of STZ is presented in Fig. 5. All parameters are given in Table 2.
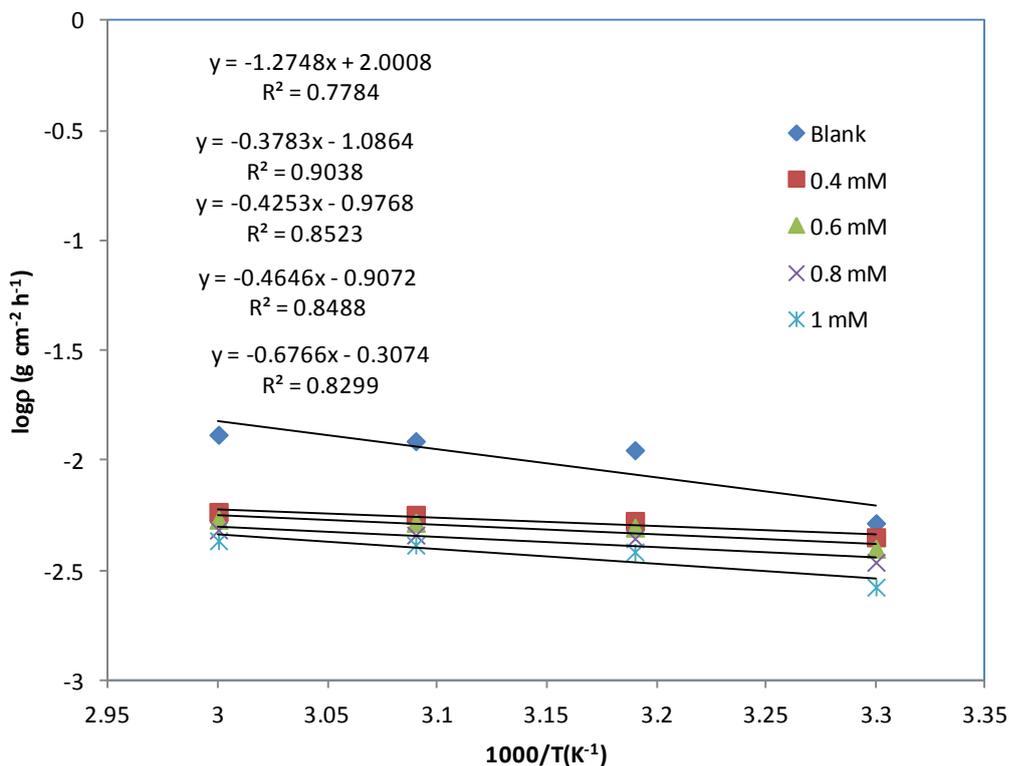

Figure 5. Arrhenius plot for mild steel corrosion in 0.5 M HCl in the absence and presence of different concentrations of sulphathiazole (STZ).

The relationship between the temperature dependence of percent inhibition efficiency *(%I)* of an inhibitor and the activation energy found in its presence was given as follows [27]:

(i) Inhibitors whose *(%I)* decreases with temperature increase. The value of activation energy *(Ea)* found is greater than that in the uninhibited solution. (ii) Inhibitors whose *(%I)* does not change with temperature variation. The activation energy *(Ea)* does not change with the presence or absence

of inhibitors. (iii) Inhibitors whose *(%I)* increases with temperature increase. The value of activation energy (*Ea*) found is less than that in the uninhibited solution. While the higher value of the activation energy (*Ea*) of the process in an inhibitor's presence when compared to that in its absence according to Ebenso et al. [43] is attributed to its physical adsorption, its chemisorptions is pronounced in the opposite case [41]. The lower value of *Ea* in the presence of STZ compared to that in its absence and the increase of %*I* with temperature increase can be interpreted as an indication of chemical adsorption.

Table 2. Activation parameters of the dissolution of mild steel in 0.5 M HCl in the absence and presence of different concentrations of STZ.

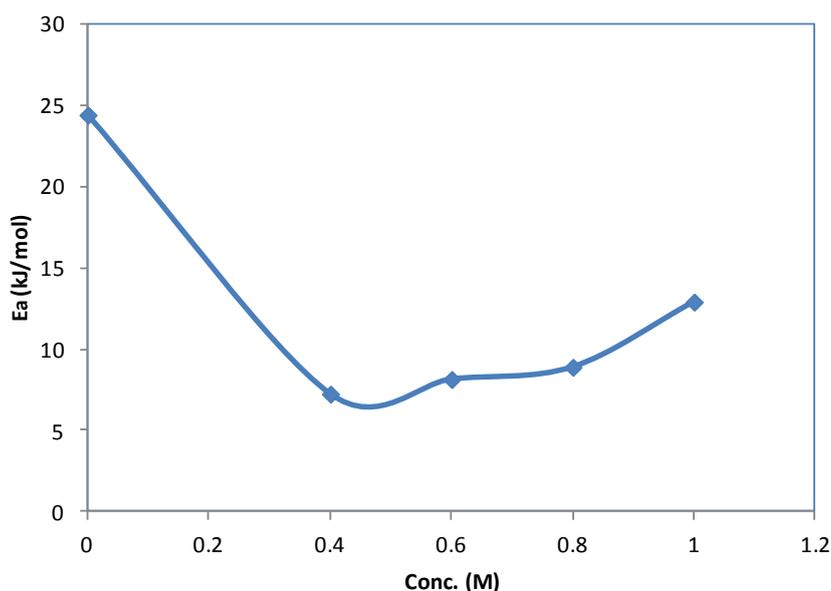| Conc.	A (g cm^{-2} h^{-1})	E^a (kJ mol^{-1})
Blank	100.18	24.40
0.4 mM	0.08	7.24
0.6 mM	0.11	8.14
0.8 mM	0.12	8.89
1.0 mM	0.49	12.9

Figure 6. Variation of activation energy, *Ea,* with the concentrations of STZ.

Fig. 6 represents the variation of *Ea* with STZ concentration. As can be observed, increasing the amount of STZ leads to an abrupt decrease in the activation energy up to a minimum value at 0.4

mM and then it increases slightly with increase in STZ concentration. However, even at the deflection point, the *Ea* values are quite lower than that obtained for the uninhibited solution which supports the mechanism of chemisorption earlier proposed.

3.3. Adsorption isotherm and thermodynamic parameters

It has been assumed that inhibitor molecules establish their inhibition action via the adsorption of the inhibitor onto the metal surface [44]. The adsorption can be described by two main types of interaction: physical adsorption and chemisorption. The adsorption processes of inhibitors are influenced by the chemical structure of organic compounds, the nature and surface change of metal, the distribution of charge in molecule, and the type of aggressive media [1, 45]. The efficiency of drugs like sulphathiazole as a corrosion inhibitor mainly depends on its adsorption ability at the metal/solution interface. Therefore, it is essential to know the mode of adsorption and the adsorption isotherm that can give valuable information about the interaction of inhibitor and metal surface. The values of surface coverage (θ) [$\%I = 100 \times \theta$] calculated for different concentrations of STZ were used to test graphically to various adsorption isotherms including Freundlich, Langmuir, Temkin and Frumkin isotherms. To choose the isotherm that best fit the experimental data, the correlation coefficient (R^2) was used and the best fit was obtained from the Temkin isotherm, which can be expressed by the following equation:

$$\exp(-2\alpha\theta) = K_{ads}C \tag{4}$$

where the molecular interaction parameter α can have both positive and negative values. Positive values of α indicate attraction forces between the adsorbed molecules while negative values indicate repulsive forces between the adsorbed molecules [42]. Upon rearrangement of Eq. (4), the following equation is obtained:

$$\theta = [1/(-2\alpha)]\ln(K_{ads}C) \tag{5}$$

If the parameter f is defined as:

$$f = -2\alpha \tag{6}$$

where f is the heterogeneous factor of the metal surface describing the molecular interactions in the adsorption layer and the heterogeneity of the metal surface. Eq.(6) clearly shows that the sign between f and α is reverse, that is, if $\alpha < 0$, then $f > 0$; if $\alpha > 0$, then $f < 0$. Accordingly, if $f > 0$, mutual repulsion of molecules occurs and if $f < 0$ attraction takes place. If Eq. (6) is substituted into Eq. (5), then the Temkin isotherm equation has the following form:

$$\theta = (1/f)\ln(K_{ads}C) \tag{7}$$

Eq. (7) can be transformed into:

$$\theta = (1/f) \ln K_{ads} + (1/f) \ln C \qquad (8)$$

Eq.(8) is a different form of the Temkin isotherm. The plot of θ versus *ln C* gives a straight line graph with a slope of *(1/f)* and an intercept of *[(1/f)ln K_{ads}]*. It is clear that *f* can be calculated from the slope, with the calculated *f*, the value of K_{ads} can be obtained from the intercept. All the parameters are listed in Table 3.

Table 3. Some parameters from Temkin isotherm model for mild steel in 0.5 M HCl.

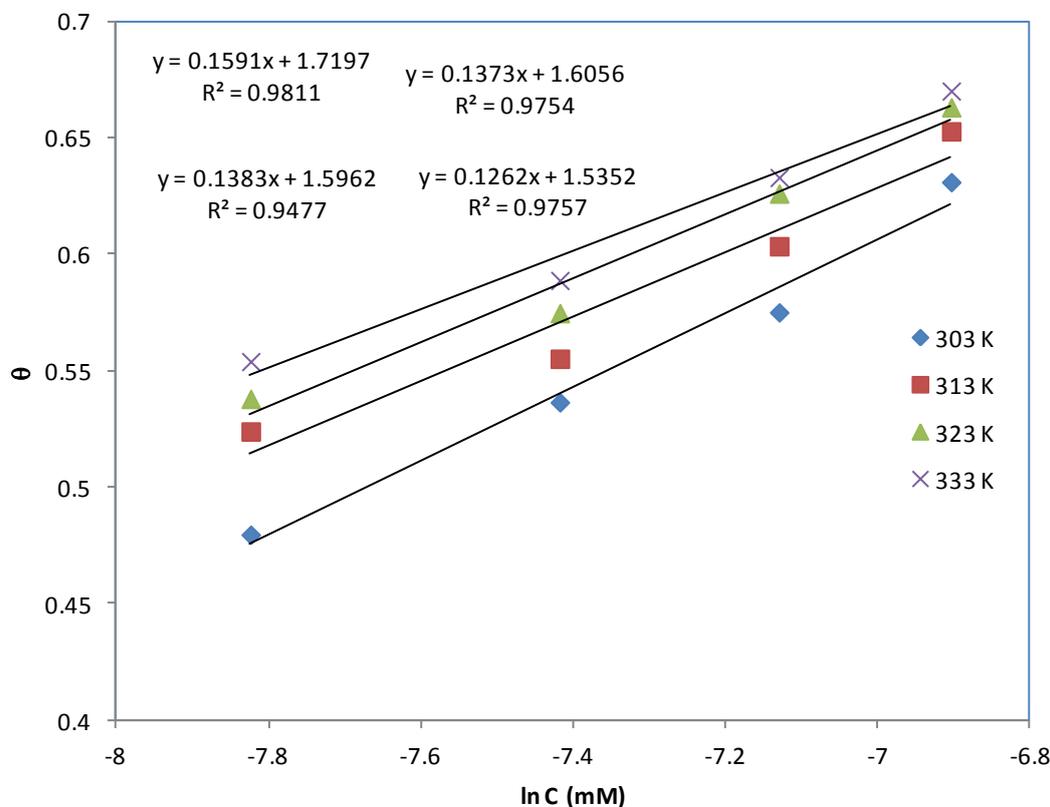| Temperature (K)	f	K_{ads} (M^{-1})	(R^2)	ΔG^o_{ads} (kJ mol^{-1})
303	6.28	49020	0.981	-37.32
313	7.23	102744	0.947	-40.48
323	7.28	119372	0.975	-42.17
333	7.92	190994	0.975	-44.78

Figure7. The relationship between θ and *ln C* at different temperatures.

Fig. 7, shows the relationship between θ and *ln C* at different temperatures. These results show that all the linear correlation coefficients (R^2) are close to 1, which indicates that the adsorption of STZ

onto steel surface obeys the Temkin adsorption isotherm. Furthermore, it can be deduced that there is repulsion force in the adsorption layer due to $f > 0$. In literature, it was reported that the value of $K_{ads} > 100$ M^{-1} is attributed to a stronger and more adsorbed layer formation on the metal surface [46]. Therefore, large values of K_{ads} obtained in this work (Table 3), mean better inhibition efficiency of the inhibitor, i.e., strong electrical interaction between the double-layer existing at the phase boundary and the adsorbing inhibitor molecules [46].

K_{ads} is related to the free energy of adsorption ΔG_{ads}^{o} by the equation [47]:

$$\log K_{ads} = -\log C_{H_2O} - \frac{\Delta G_{ads}^{o}}{2.303RT} \qquad (9)$$

where C_{H2O} is the concentration of water expressed in mol/L (the same as that of inhibitor concentration), R is the molar gas constant (*J mol^{-1}K^{-1}*) and *T* is the absolute temperature *(K)*.

Calculated free energies ΔG_{ads}^{o} values are given also in Table 3. The negative values of ΔG_{ads}^{o} indicate spontaneous adsorption of STZ onto the mild steel surface [48] and strong interactions between inhibitor molecules and the metal surface [49]. Generally, values of ΔG_{ads}^{o} up to -20 kJ mol^{-1} are consistent with physisorption, while those around -40 kJ mol^{-1} or higher are associated with chemisorption as a result of the sharing or transfer of electrons from organic molecules to the metal surface to form a coordinate bond [50]. The calculated values of ΔG_{ads}^{o} are around -40 kJ mol^{-1}, indicating that the adsorption mechanism of STZ on mild steel in 0.5 M HCl solution at the studied temperatures is chemisorption [41]. The unshared electron pairs in nitrogen atoms may interact with d-orbitals of Fe to provide a protective chemisorbed film [51]
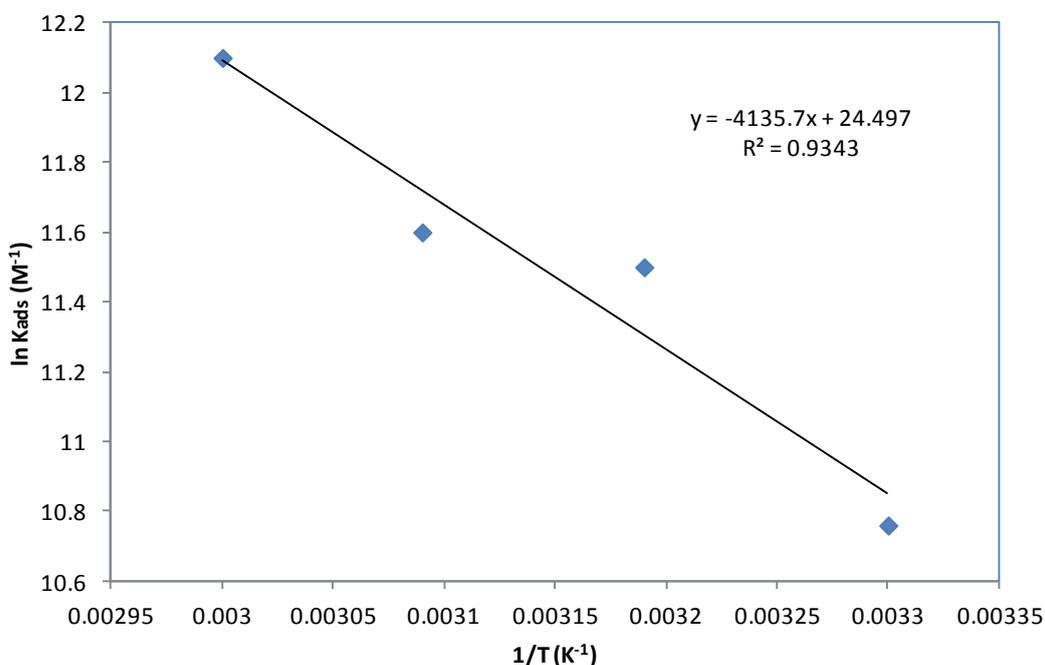

Figure 8. The relationship between lnK_{ads} and *1/T*

Thermodynamic parameters such as enthalpy of adsorption ΔH^o_{ads} and entropy of adsorption ΔS^o_{ads} can be deduced from integrated version of the Van't Hoff equation expressed by [52]:

$$\ln K_{ads} = -\frac{\Delta H^o_{ads}}{RT} + \frac{\Delta S^o_{ads}}{R} + \ln \frac{1}{55.5} \qquad (10)$$

Fig. 8 shows the plot of lnK_{ads} versus $1/T$ which gives straight lines with slope of ($-\Delta H^o_{ads}/R$) and intercepts of ($\Delta S^o_{ads}/R + \ln 1/55.5$). Calculated value of ΔH^o_{ads} and ΔS^o_{ads} using the Van't Hoff equation are 34.4 kJ mol^{-1} and 237.0 J mol^{-1} K^{-1} respectively.

The enthalpy and entropy for the adsorption of STZ on mild steel were also deduced from the thermodynamic basic equation [53]:

$$\Delta G^o_{ads} = \Delta H^o_{ads} - T\Delta S^o_{ads} \qquad (11)$$

where ΔH^o_{ads} and ΔS^o_{ads} are the enthalpy and entropy changes of adsorption process, respectively. A plot of ΔG^o_{ads} versus T was linear (Fig. 9) with the slope equal to $-\Delta S^o_{ads}$ and intercept of ΔH^o_{ads}.

Figure 9. The relationship between ΔG^o_{ads} and Temperature.

The enthalpy of adsorption ΔH^o_{ads}, and the entropy of adsorption ΔS^o_{ads}, obtained are 35.3 kJ mol^{-1} and 240.0 J mol^{-1} K^{-1} respectively. The enthalpy of adsorption ΔH^o_{ads} and entropy of adsorption ΔS^o_{ads} obtained from the two approaches are in agreement.

It has been reported that an endothermic adsorption process ($\Delta H^o_{ads} > 0$) is due to chemisorption while an exothermic adsorption process ($\Delta H^o_{ads} < 0$) may be attributed to physisorption, chemisorption or a mixture of both [54]. The positive value of enthalpy of adsorption supports the mechanism of chemisorption proposed earlier. The positive sign of ΔS^o_{ads} could be explained as follows: the adsorption of organic inhibitor molecules from the aqueous solution can be regarded as a quasi-substitution process between the organic compound in the aqueous phase $Org_{(sol)}$ and the water molecules on the metallic surface $H_2O_{(sol)}$ [55]:

$$Org_{(sol)} + xH_2O_{(ads)} \rightarrow Org_{(ads)} + xH_2O_{(sol)} \qquad (12)$$

where $Org_{(sol)}$ and $Org_{(ads)}$ are the organic molecules in the aqueous phase and adsorbed on the metallic surface, respectively, $H_2O_{(ads)}$ is the water molecules on the metallic surface, and x is the size ratio representing the number of water molecules replaced by one molecule of organic adsorbate. In this investigation, the adsorption of STZ is accompanied by desorption of water molecules from the surface of steel. Therefore, the positive value of ΔS^o_{ads} obtained in this study is attributed to the increase in solvent entropy and to a more positive water desorption enthalpy obtained [56]. The positive value of ΔS^o_{ads} also means an increase in disorderliness takes place in going from the reactants to the metal/solution interface [41], which is the driving force for the adsorption of STZ onto the steel surface.

3.4. Quantum chemical studies

Recently, the density functional theory (DFT) has been used to analyze the characteristics of the inhibitor/surface mechanism and to describe the structural nature of the inhibitor on the corrosion process [57, 58]. Furthermore, DFT is considered a very useful technique to probe the inhibitor/surface interaction as well as to analyze the experimental data.

B3LYP, a version of the DFT method that uses Becke's three parameter functional (B3) and includes a mixture of HF with DFT exchange terms associated with the gradient corrected correlation functional of Lee, Yang and Parr (LYP) [59], was used in this paper to carry out quantum calculations. Then, full geometry optimization together with the vibrational analysis of the optimized structures of the inhibitor was carried out at the (B3LYP/6-31G (d) level of theory using Gaussian 03 program package [60] in order to determine whether they correspond to a minimum in the potential energy curve. Thus in the present investigation, quantum chemical calculation using DFT was employed to explain the experimental results obtained in this study and to further give insight into the inhibition action of STZ on the mild steel surface.

According to the description of frontier orbital theory, HOMO is often associated with the electron donating ability of an inhibitor molecule. High E_{HOMO} values indicate that the molecule has a tendency to donate electrons to the metal with unoccupied molecule orbitals. E_{LUMO} indicates the ability of the molecules to accept electrons [3]. The lower value of E_{LUMO} is the easier acceptance of electrons from metal surface [42]. The gap between the LUMO and HOMO energy levels of the

inhibitor molecules is another important index, the low absolute values of the energy band gap ($\Delta E = E_{LUMO} - E_{HOMO}$) means good inhibition efficiency [51]. Table 4 presents the calculated quantum parameters for STZ. The optimized equilibrium structure is shown in Fig. 10.
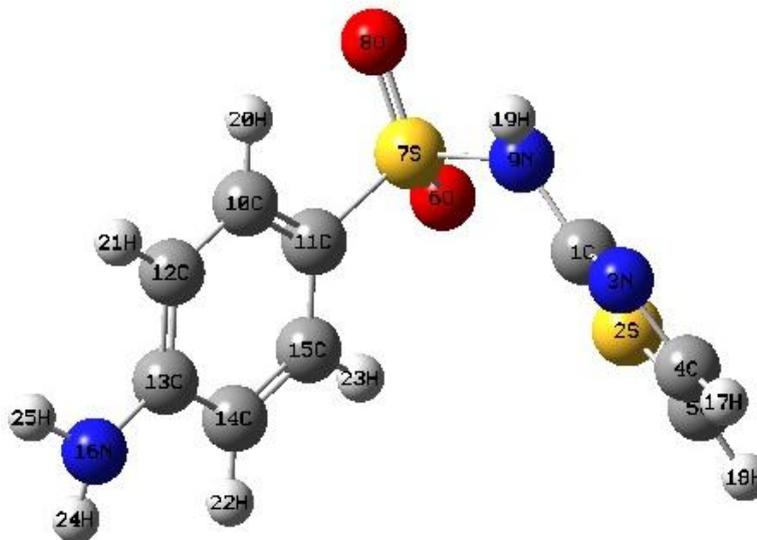

Figure 10. Optimized structure of sulphathiazole

The data listed in Table 4 verified that STZ has high value of E_{HOMO} and low value of E_{LUMO} with low energy band gap which supports its inhibition action on steel surface.

Table 4. Molecular properties of STZ calculated using DFT at the B3LYP/6-31G (d) basis set.

E_{HOMO} (eV)	E_{LUMO} (eV)	ΔE (eV)	μ (D)	ΔN	η	ΔE_T
-0.221	-0.036	0.185	6.960	36.44	0.092	-0.023

The fraction of electrons transferred from the inhibitor molecule to the metallic atom *(ΔN)* was also calculated in the present study [61]. The idea behind this is that in the reaction of two systems with different electronegativities (as a metallic surface and an inhibitor molecule) the following mechanism will take place: the electron flow will happen from the molecule with the low electronegativity towards that of a higher value, until the chemical potentials are the same. In order to calculate the fraction of electrons transferred, a theoretical value for the electronegativity of bulk iron was used χ_{Fe} =7eV, and a global hardness of η_{Fe} = 0, by assuming that for a metallic bulk $I = A$ because they are softer than the neutral metallic atoms. For the calculation the following formula was used [42].

$$\Delta N = \frac{\chi_{Fe} - \chi_{inb}}{2(\eta_{Fe} + \eta_{inh})} \tag{13}$$

These quantities are related to electron affinity (A) and ionization potential (I) which are useful in their ability to help predict chemical behavior [61].

$$\chi = \frac{I + A}{2} \tag{14}$$

$$\eta = \frac{I - A}{2} \tag{15}$$

I and A are related in turn to E_{HOMO} and E_{LUMO} as follows:

$$I = -E_{HOMO} \tag{16}$$

$$A = -E_{LUMO} \tag{17}$$

The fraction of electrons transferred from inhibitor to the mild steel surface ΔN, was calculated and listed also in Table 4. According to Lukovits, if $\Delta N < 3.6$, the inhibition efficiency increased with increasing electron donating ability at the metal surface [62]. In this study, the value of ΔN for STZ was greater than 3.6 which shows that the increase in inhibition efficiency was not due to solely the electron donating ability of STZ.

Thus, the simple charge transfer model for donation and back donation of charges proposed recently by Gomez et al., [63], can be applied for the present study. According to this model, when the molecule receives a certain amount of charge, ΔN^+;

$$\Delta E^+ = \mu^+ \Delta N^+ + \frac{1}{2}\eta(\Delta N^+)^2 \tag{18}$$

while when the molecule back-donates a certain amount of charge, ΔN^-, then:

$$\Delta E^- = \mu^- \Delta N^- + \frac{1}{2}\eta(\Delta N^-)^2 \tag{19}$$

If the total energy change is approximated by the sum of the contributions of Eqs. (18) and (19), and assuming that the amount of charge back-donation is equal to the amount of charge received, $\Delta N^- = -\Delta N^+$, then;

$$\Delta E_T = \Delta E^+ + \Delta E^- = (\mu^+ - \mu^-)\Delta N^+ + \eta(\Delta N^+)^2 \tag{20}$$

The most favourable situation corresponds to the case when the total energy change becomes a minimum with respect to ΔN^+, which implies that $\Delta N^+ = -(\mu^+ - \mu^-)/2\eta$ and that;

$$\Delta E_T = -(\mu^+ - \mu^-)^2 / 4\eta = -\eta / 4 \tag{21}$$

The calculations from Table 4 indicate that $\eta > 0$ (η = hardness) and $\Delta E_T < 0$. This result implies that the charge transfer to a molecule followed by back-donation from the molecule is energetically favourable and is responsible for the inhibitive effect of STZ. Similar observation has been reported [42, 64].
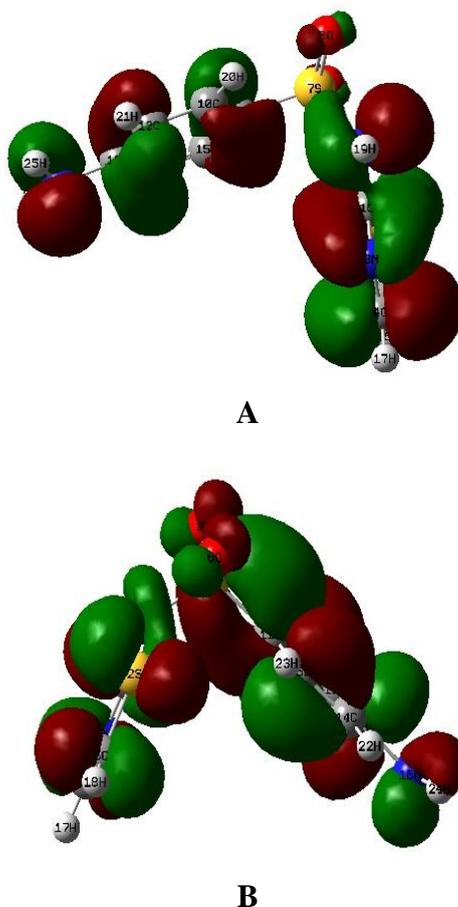
Table 5. Mulliken charge density of the STZ molecule

Atom	Charges
C1	0.251784
S2	0.285361
N3	-0.426187
C4	0.057357
C5	-0.358390
O6	-0.535656
S7	1.199732
O8	-0.525230
N9	-0.704376
C10	-0.150302
C11	-0.152645
C12	-0.167516
C13	0.337415
C14	-0.168754
C15	-0.146070
N16	-0.790073

The Mulliken charge distribution of STZ is presented in Table 5. It has been reported that the more negative the atomic charges of the adsorbed centre, the more easily the atom donates its electron to the unoccupied orbital of the metal [65]. It could be readily observed that nitrogen, oxygen and some carbon atoms have high charge densities. The regions of highest electron density are generally the sites to which electrophiles can attack [66]. Therefore, N, O and some C atoms were the active centers, which had the strongest ability of bonding to the metal surface. On the other hand, sulphur and some carbon atoms carry positive charges, which are sites to which nucleophiles can attack. Therefore, STZ can accept electrons from Fe through these atoms. It has been reported that excellent corrosion inhibitors can not only offer electrons to unoccupied orbital of the metal, but also accept free electrons from the metal. These strengthens the chemisorption of STZ on steel surface leading to a stable protective layer and thus, retarding further corrosion of the metal in hydrochloric acid solution.

From Fig. 11, it could be seen that STZ have similar HOMO and LUMO distributions, which were all located on the entire sulphathiazole moiety. This is due to the presence of nitrogen, oxygen

and carbon atoms together with several π-electrons on the entire molecule. Thus, the unoccupied d orbitals of Fe atom can accept electrons from inhibitor molecule to form coordinate bond. Also the inhibitor molecule can accept electrons from Fe atom with its anti-bonding orbitals to form back-donating bond.

A

B

Figure 11. The frontier molecular orbital density of STZ: (a) HOMO and (b) LUMO

4. CONCLUSIONS

1.   STZ acts as a good inhibitor for the corrosion of mild steel in 0.5 M HCl.

2.   Inhibition efficiency increases with increase in the concentration of the studied inhibitor and with rise in temperature.

3.   The adsorption of STZ on the steel surface obeys the Temkin adsorption isotherm. Furthermore, the obtained values of ΔG^{o}_{ads} indicate that the adsorption of STZ molecules onto the steel surface was a spontaneous process and typical of chemisorption.

4.   The activation energy and the enthalpy of adsorption values obtained also confirm the chemical nature of the interaction between STZ and the steel surface.

5.   Quantum chemical calculations show that STZ adsorbed mainly as molecular species on the steel surface using nitrogen, oxygen and some carbons atoms as its active centers.

References

1. I. Ahamad, R. Prasad, M. A. Quraishi, *Corros. Sci.* 52 (2010) 933.
2. A. Y. Musa, A. H. Kadhum, A. B. Mohamad, M. F. Takriff, E. P. Chee, *Curr. Appl. Phys.* 12 (2012) 325.
3. I.B. Obot, N.O. Obi-Egbedi, *Curr. Appl. Phys*. 11 (2011) 382.
4. S. Ghareba, S. Omanovic, *Corros. Sci.* 52 (2010) 2104.
5. A. Y. Musa, A. H. Kadhum, A. B. Mohamad, A. B. Rahoma, H. Mesmari, *J. Mol. Struct.* 969 (2010) 233.
6. S. John, B. Joseph, K. V. Balakrishnan, K. K. Aravindakshan, A. Joseph, *Mater. Chem. Phys*. 123 (2010) 218.
7. A. E. Fouda, A. Al-Sarawy, E. El-Katori, *European. J. Chem.* 1(4) (2010) 312.
8. S. E. Nataraja, T. V. Venkatesha, K. Manjunatha, B. Poojary, M. K. Pavithra, H. C. Tandon, *Corros. Sci.* 53 (2011) 2651.
9. A. K. Singh, M. A. Quraishi, *Corros. Sci.* 52 (2010) 1373.
10. S. A. Ali, A. M. El-Shareef, R. F. Al-Ghamdi, M. T. Saeed, *Corros. Sci.* (2011) 2651.
11. H. Ju, Y. Li, *Corros. Sci.* 49 (2007) 4185.
12. A. Kokalj, *Electrochim. Acta* 53 (2011) 745.
13. J.J. Fu, S.N. Li, L.H. Cao, Y.Wang, L.H. Yan, L.D. Lu, *J. Mater. Sci*. 45 (2010) 979.
14. S.K. Shukla, A.K. Singh, I. Ahamad, M.A. Quraishi, *Mat. Lett*. 63 (2009) 819.
15. S.K. Shukla, M.A. Quraishi, *Corros. Sci*. 51 (2009) 1007.
16. M.M. Solomon, S.A. Umoren, I.I. Udousoro, A.P. Udoh, *Corros. Sci*. 52 (2010) 1317.
17. M. Forsyth, M. Seter, B. Hinton, G. Deacon, P. Junk, *Australian J. Chem.* 64(6) (2011) 812.
18. H. Ashassi-Sorkhabi, M.R. Majidi, K. Seyyedi, *Appl. Surf. Sci*. 225 (2004) 176.
19. M. A. Amin, *Corros. Sci.* 52 (2010) 3243.
20. G. Gece, S. Bilgic, *Corros. Sci.* 52 (2010) 3435.
21. A.S. Fouda, H.A. Mostafa, H.M. El-Abbasy, *J. Appl. Electrochem.* 40 (2010) 163.
22. M. Abdallah, *Corros. Sci.* 44 (2002) 717.
23. E.E. Ebenso, T. Arslan, F. Kandemirli, N. Caner, I. Love, *Int. J. Quantum Chem*. 110 (2010) 1003.
24. G. Gece, *Corros. Sci*. 53 (2011) 3873.
25. I.B. Obot, N.O. Obi-Egbedi, S.A. Umoren, E.E. Ebenso, *Chem. Eng. Comm.* 198 (2011) 711.
26. I.B. Obot, N.O. Obi-Egbedi, *Corros. Sci.* 52 (2010) 198.
27. I.B. Obot, N.O. Obi-Egbedi, S.A. Umoren, *Corros. Sci. 51* (2009) 1868.
28. T. Arslan, F. Kandemirli, E. E. Ebenso, I. Love, H. Alemu, *Corros. Sci.* 51 (2009) 35.
29. I.B. Obot, and N.O. Obi-Egbedi, *Corros. Sci*. 52 (2010) 282.
30. I.B. Obot, N.O. Obi-Egbedi, *Mater. Chem. Phys*. 122 (2010) 325.
31. N.O.Obi-Egbedi, I.B. Obot, *Arab. J. Chem*. 2010, doi: 10.1016/j.arabjc.2010.08.004.
32. A.A. Khadom, A.S. Yaro, A.H. Kadum, *J. Taiwan. Inst. Chem. Engr*. 41 (2010) 122.
33. A.A. Rahim, J. Kassim, *Recent. Patents Mater. Sci.* 1 (2008) 223.
34. S.K. Shukla, A.K. Singh, I. Ahamad, M.A. Quraishi, *Mat. Lett*. 63 (2009) 819.
35. S.K. Shukla, M.A. Quraishi, *Corros. Sci*. 51 (2009) 1007.
36. S.A. Umoren, I.B. Obot, *Surf. Rev. Lett*. 15(3) (2008), 277.
37. S.A. Umoren, I.B. Obot, E.E. Ebenso, N.O. Obi-Egbedi, *Desalination* 247 (2009), 561.
38. Y. Abboud, A. Abourriche, T. Saffaj, M. Berrada, M. Charrouf, A. Bennamara, H. Hannache, *Desalination* 247 (2009) 175.

39. J. Zhao, N. Zhang, C. Qu, X. Wu, J. Zhang, X. Zhang, *Ind. Eng. Chem. Res*. 49 (2010) 3986.
40. A. Fouda, A. Al-Sarawy, E. El-Katori, *European. J. Chem*. 1(4) (2010) 312.
41. X. Li, S. Deng, H. Fu, T. Li, *Electrochim. Acta* 54 (2009) 4089.
42. I. B. Obot, N. O. Obi-Egbedi, A.O. Eseola, *Ind. Eng. Chem. Res.* 50 (2011) 2098.
43. E.E. Ebenso, H. Alemu, S.A. Umoren, I.B. Obot, *Int. J. Electrochem. Sci.* 4 (2008) 1325.
44. E. Machnikova, K. H. Whitmire, N. Hackerman, *Electrochim. Acta* 53 (2008) 6024.
45. I. Ahamad, R. Prasad, M. A. Quraishi, *Corros. Sci*. 52 (2010) 933.
46. I. Ahamad, R. Prasad, M.A. Quraishi, *Mater. Chem. Phys*. 124 (2010) 1155.
47. G. Avci, *Colloids & Surf.A: Physicochem. Eng. Aspects* 317 (2008) 730.
48. H. Ashassi-Sorkhabi, B. Shaabani, D. Seifzadeh, *Appl. Surf. Sci*. 239 (2005) 154.
49. M.M. Solomon, S.A. Umoren, I.I. Udousoro, A.P. Udoh, *Corros. Sci*. 52 (2010) 1317.
50. N.O. Obi-Egbedi, I.B. Obot, *Corros. Sci*. 53 (2011) 282.
51. I.B. Obot, N.O. Obi-Egbedi, *Corros. Sci.* 52 (2010) 657.
52. E.A. Noor, *J. Appl. Electrochem.* 39 (2009) 1465.
53. A.M. Badiea, K.N. Mohana, *Corros. Sci.* 51 (2009) 2231.
54. N.O. Obi-Egbedi, I.B. Obot, A.O. Eseola, *Arab. J. Chem*. 2010, doi: 10.1016/j.arabjc.2010.10.025.
55. G. K. Gomma, M. H. Wahdan, *Mater. Chem. Phys.* 39 (1994) 420.
56. I.B. Obot, N.O. Obi-Egbedi, *Colloids & Surf.A: Physicochem. Eng. Aspects* 330 (2008) 2007.
57. M. Lashkari, M. R. Arshadi, *J. Chem. Phys*. 299 (2004) 131.
58. L.T. Sein, Y. Wei, S.A. Jansen, *Comput. Theor. Polym. Sci.* 11 (2001) 83.
59. C. Lee, W. Yang, RG. Parr, *Phys. Rev. B37* (1988) 785.
60. M.J. Frisch, G.W. Trucks, H.B. Schlegel, G.E. Scuseria, M.A. Robb, J.R. Cheeseman Jr., J.A. Montgomery, T. Vreven, K.N. Kudin, J.C. Burant, J.M. Millam, S.S. Iyengar, J. Tomasi, V. Barone, B. Mennucci, M. Cossi, G. Scalmani, N. Rega, G.A. Petersson, H. Nakatsuji, M. Hada, M. Ehara, K. Toyota, R. Fukuda, J. Hasegawa, M. Ishida, T. Nakajima, Y. Honda, O. Kitao, H. Nakai, M. Klene, X. Li, J.E. Knox, H.P. Hratchian, J.B. Cross, V. Bakken, C. Adamo, J. Jaramillo, R. Gomperts, R.E. Stratmann, O. Yazyev, A.J. Austin, R. Cammi, C. Pomelli, J.W. Ochterski, P.Y. Ayala, K. Morokuma, G.A. Voth, P. Salvador, J.J. Dannenberg, V.G. Zakrzewski, S. Dapprich, A.D. Daniels, M.C. Strain, O. Farkas, D.K. Malick, A.D. Rabuck, K. Raghavachari, J.B. Foresman, J.V. Ortiz, Q. Cui, A.G. Baboul, S. Clifford, J. Cioslowski, B.B. Stefanov, G. Liu, A. Liashenko, P. Piskorz, I. Komaromi, R.L. Martin, D.J. Fox, T. Keith, M.A. Al-Laham, C.Y. Peng, A. Nanayakkara, M. Challacombe, P.M.W. Gill, B. Johnson, W. Chen, M.W. Wong, C. Gonzalez, J.A. Pople, Gaussian 03W, Gaussian Inc., Wallingford CT, 2004.
61. A. Y. Musa, A. H. Kadhum, A. B. Mohamad, M. F. Takriff, E. P. Chee, *Mater. Chem. Phys.* (2011), doi: 10.1016/j.matchemphys.2011.05.010.
62. J. Fu, S. Li, Y. Wang, *J. Mater. Sci.* 45 (2010) 6255.
63. B. Gomez, N.V. Likhhanova, M.A. Dominguez-Aguilar, R. Martinez-Palou, A.Vela, J.L. Gazquez, *J. Phys. Chem. B* 110 (2006) 8928.
64. N.O. Obi-Egbedi, I.B. Obot, M.I. El-Khaiary, *J. Mol. Struct.* 1002 (2011) 86.
65. S. Xia, M. Qiu, L. Yu, F. Liu, H. Zhao, *Corros. Sci.* 50 (2008) 2021.
66. A.Y. Musa, A. H. Kadhum, A. B. Mohamad, A. B. Rahoma, H. Mesmari, *J. Mol. Struct.* 969 (2010) 233.